Anterior Dislocation of Glenohumeral Joint: Quantitative Analysis of the Dynamic Stabilizers

Ehsan Sarshari[1]

[1]

Abstract— **The etiology behind the shoulder anterior instability is defined through quantitative analysis of the dynamic stabilizers of the shoulder. To this end, a mathematical model of the shoulder including all the major muscles spanning the glenohumeral joint is derived and verified with the measured *in vivo* data. The results show that the active anterior stability diminishes during the end-range motions which can lead to anterior dislocation if the passive structures are dysfunctional.**

Keywords— **glenohumeral joint, anterior dislocation, active stabilizers, vector analysis.**

I. Introduction

Given the most extensive range of motion exhibited by glenohumeral joint of any joint in our body, it lacks inherent osseous stability. Anterior instability accounts for almost 95% of the shoulder dislocations [1]. The current concepts of glenohumeral joint stability can be broadly separated into two main spectrums. Some espouse the joint sacrifices stability for mobility [2] and conversely, others advocate the joint is a perfect compromise of mobility and stability [3]. Fewer studies quantitatively have discussed the joint stability utilizing biomechanical models. In [4] a biomechanical model was utilized to assess the muscle contributions toward stability of the joint. Other studies were mainly utilized either purely clinical [5–7] or cadaveric [8–10] approaches to address the joint stability.

The glenohumeral joint stability is accomplished through sophisticated coordination amongst different mechanisms, mainly divided into passive as well as active structures. These structures are all aimed at assisting the stability by predisposing the humeral head to concentric motion. These stability structures were thoroughly reviewed in [2, 3]. The available articulation area is enhanced based on increase in the arm elevation which affects the joint stability in the end-range [11]. Although the ambiguous function of labrum, it seems to serve to increase the contact surface [12]. Longhead of biceps brachii has also a stabilizing role to play solely in the mid-range, prescribing the optionality in considering the arm while investigating the end-range stability of glenohumeral joint [13]. The collagen fibers allow the capsuloligamentous to act as a damper in the end-range and significantly absorb the exerted stress and tension [14, 15]. Intraarticular pressure may also cooperate in slightly enhancing the stability in extreme postures [16]. Neuromuscular structures which are perceived as the prime active stabilizers contribute to the joint stability by pressing the humeral head against the glenoid fossa [4].

As highlighted above, the action of these mechanisms varies along the arm position. The present study is aimed at quantitatively assessing the operation of active stabilizers. To this end, the contributions of muscles as the dynamic stabilizers of the shoulder are assessed through the line of actions and the locus of their applied forces on the glenoid fossa.

The paper is organized as follows. In Section II. the model is transparently developed and is partially validated. Section III. deals with quantifying the function of active stabilizers. The results are also discussed at the same section in the sense of curtness. Eventually, the argument will be concluded in Section IV.

II. Methods

The model is clearly described in Fig. 1. It consists of a rigid body, representing the humerus, and the scapula which its motion is considered by scapulohumeral rhythm of 2:1 for the abduction angles above 30° [17]. The humeral head was approximated by a sphere [18]. All the major muscles crossing the glenohumeral joint are included in the model as massless taut ropes: the anterior deltoid (AD), the middle deltoid (MD), the posterior deltoid (PD), the supraspinatus (SS), the infraspinatus together with the treres minor (IS), and the subscapularis (SC). Two separate embedded coordinates are considered for scapula and humerus distinguished by A^S and A^H, respectively. The inertia frame is denoted by A^T. The scapula coordinate was centered at the center of the sphere approximates the glenoid fossa [18].

A. Wrapping

The path taken by the muscle implies the line of action and the moment arm of the muscle force that their key effects on the model outcome have been already highlighted [19]. During the joint motion the muscle path might be interrupted by bony obstacles and cannot therefore be represented as a straight line connecting the origin to the insertion. The path should thus be wrapped around the interfering bony contours.

The developed wrapping methodologies can be widely divided into geometrical and optimization based methods, described in [20]. The geometrical wrapping method utilized in this study borrows the main idea from [20] although it has

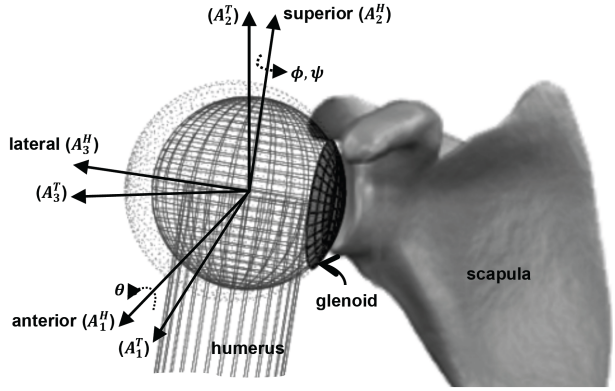

Fig. 1: general configuration of the model.

been established in a more transparent fashion. Fig. 2 illustrates the trajectory of an arbitrary muscle element wrapped over the humeral head and serves to introduce some notations.

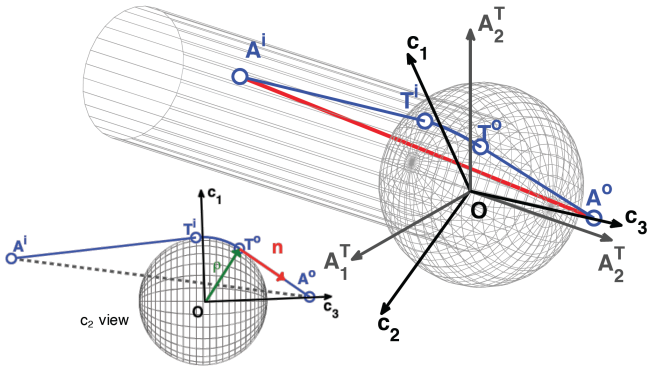

Fig. 2: muscle path is wrapped around the offending structure.

Following the approximation that no friction acts between the massless muscle rope and the obstacle surface, it can be deduced from force balance of the differential elements of the muscle rope that the path always lies on the surface defined by the origin, the insertion, and humeral head center. The idea is to find a unique rotation matrix that relates the humeral-fixed frame (A^H) to an intermediate frame C, with associated coordinate axes $c_1c_2c_3$, in which the muscle via point (T^o) remains unchanged. The frame C could be therefore achieved by applying a sequence of rotations through which the above-defined surface coincides with the c_1c_3 surface. The successive rotations relate A^H to C are outlined in Algorithm 1.

Having defined the coordinate of via point T^o, the moment arm $\boldsymbol{\rho}$ and the unit vector $\boldsymbol{n}$ corresponding to the line of action can be simply defined in C which can be then transformed to A^H by ${}^{A^H}R^{\,C}$.

Wrapping condition. The bony contour does not always cause the muscle to be wrapped and the wrapping condition therefore serves to decide the necessity of wrapping for a given arm posture. The condition is then to check the penetration of the straight trajectory from $\boldsymbol{A}^o$ to $\boldsymbol{A}^i$ into the interfering structure (humeral head sphere). Intersecting the vector equations of the straight trajectory and the obstacle, Algorithm 2 serves to outline the wrapping condition.

Algorithm 1. defining the rotation matrix ${}^{A^H}R^{\,C}$ to map A^H to C.

set the points A^o and A^i in the corresponding frames for any arm posture.
and define

1. α around a_3^H axis: $\cos\alpha = {}^{a_1^o}/_{\sqrt{a_1^{o2}+a_2^{o2}}}$.
2. β around a_2^H axis: $\cos\beta = {}^{a_3^o}/_{|A^o|}$.
3. ${}^nA^i$ associated with A^i in the resulted frame so far.
4. γ around twice rotated a_3^H axis: $\cos\gamma = {}^{{}^na_1^i}/_{\sqrt{{}^na_1^{i\,2}+{}^na_2^{i\,2}}}$.
5. ${}^{A^H}R^{\,C} = \begin{bmatrix} c\gamma\, c\beta\, c\alpha - s\gamma\, s\alpha & -s\gamma\, c\beta\, c\alpha - c\gamma\, s\alpha & s\beta\, c\alpha \\ c\gamma\, c\beta\, s\alpha + s\gamma\, c\alpha & -s\gamma\, c\beta\, s\alpha + c\gamma\, c\alpha & s\beta\, s\alpha \\ -c\gamma\, s\beta & s\gamma\, s\beta & c\beta \end{bmatrix}$

Algorithm 2. wrapping condition.

set the unit vector $\boldsymbol{d}$ equals to $\overrightarrow{A^iA^o}/|\overrightarrow{A^iA^o}|$ in the corresponding frames for any arm posture.
and define

1. $\Delta = (d_1a_1^o + d_2a_2^o + d_3a_3^o)^2 - (a_1^{o2} + a_2^{o2} + a_3^{o2} - r^2)$.
2. $t = \frac{(a_1^o - a_1^i)a_1^o + (a_2^o - a_2^i)a_2^o + (a_3^o - a_3^i)a_3^o}{(a_1^o - a_1^i)^2 + (a_2^o - a_2^i)^2 + (a_3^o - a_3^i)^2}$.

if $\Delta \geq 0 \quad \& \quad 0 < t < 1$,
then the muscle should be wrapped.
else wrapping is not occurred.

B. *Equations of motion*

Making use of Lagrange's equations and YXY sequence of Euler angles, the equations of motion are obtained in this section. The Lagrange's equations for an unconstrained rigid body are the components of the moment balance along the nonorthogonal axes around which the Euler angle transformations were conducted [21]. In this case, the generalized forces are the components of the resultant applied external moments about the center of rotation, which were resolved in the directions of Euler angles rotations, Eq. 1.

$$\dot{\boldsymbol{L}}_O \cdot \boldsymbol{e}_i = \boldsymbol{M}_O \cdot \boldsymbol{e}_i \qquad i = \phi, \theta, \psi \tag{1}$$

where, $\boldsymbol{L}_O$ and $\boldsymbol{M}_O$ are respectively the angular momentum and resultant external moment around the humeral head center and $\boldsymbol{e}_i$ are in essence the partial velocities related to the rates of Euler angles ($\boldsymbol{e}_i = \partial\boldsymbol{\omega}/\partial\dot{q}_i$). The angular velocity vector needed to calculate $\boldsymbol{L}_O$, for the given YXY sequence in terms of the A^H frame is

$$\{\omega\} = \begin{bmatrix} \dot{\phi}\,\sin\psi\,\sin\theta + \dot{\theta}\,\cos\psi \\ \dot{\phi}\,\cos\theta + \dot{\psi} \\ -\dot{\phi}\,\cos\psi\,\sin\theta + \dot{\theta}\,\sin\psi \end{bmatrix} \tag{2}$$

Having defined the lines of action and moment arms of the muscles forces in 'Wrapping' , the resultant external moment can be written as

$$\boldsymbol{M}_O = \{M_O^{mg}\} \sum_{j=1}^{6} F_j(\boldsymbol{\rho}_j \times \boldsymbol{n}_j) \tag{3}$$

where, F_j is the magnitude of the force applied by the j^{th} muscle element, and $\boldsymbol{M}_O^{mg}$ is the moment of the gravity force calculated with respect to the humeral head center. Eq. 1 can then be rewritten as

$$(\dot{\boldsymbol{L}}_O - \{M_O^{mg}\}) \cdot \boldsymbol{e}_i = \left[\sum_{j=1}^{6} F_j(\boldsymbol{\rho}_j \times \boldsymbol{n}_j)\right] \cdot \boldsymbol{e}_i \tag{4}$$

The left side of Eq. 4 is a function of q_i, $\dot{q}_i$, and $\ddot{q}_i$. However, the right side is a function of F_j, q_i, and $\dot{q}_i$. In order to find F_j, a predefined motion (q_i, $\dot{q}_i$, and $\ddot{q}_i$) is inputted to Eq. 4, and F_j are determined in a way that these muscle forces produce the same motion (see 'Load sharing'). The matrix notation of Eq. 4 can therefore in terms of an inverse dynamic problem be rearranged as

$$\{D\} = [\boldsymbol{e}_i][W]\{F\} \tag{5}$$

where, $\{D\}_{3\times1}$ is equal to the left side of Eq. 4 and $\{F\}$ is a 6×1 vector consists of magnitude of the muscle forces. $[\boldsymbol{e}_i]$ is the partial velocities matrix, illustrated in Eq. 6 and $[W]_{3\times6}$ is called generalized moment arm matrix whose j^{th} column is $\boldsymbol{\rho}_j \times \boldsymbol{n}_j$ while j goes from 1 to 6.

$$[\boldsymbol{e}_i] = \begin{bmatrix} \sin\psi\sin\theta & \cos\theta & \sin\psi\sin\theta \\ \cos\psi & 0 & \sin\psi \\ 0 & 1 & 0 \end{bmatrix} \tag{6}$$

C. Load sharing

By denoting $[\boldsymbol{e}_i][W]$ as the quasi moment arm matrix $[B]$, Eq. 5 appears to be a linear equation, which has a solution for every $\{D\}$ if the matrix $[B]$ is full row rank. We have investigated that a viable selection of Euler sequence besides considering an anatomically consistent scapulohumeral rhythm assures to always have a solution. The complete solution of $\{D\} = [B]\{F\}$ has the form $\{F^p + F^s \mid F^s \in N(B)\}$, where p and s superscripts respectively stand for particular and special answers and $N(B)$ is the null space of $[B]$.

Three dynamic equations of Eq. 5 do not suffice to determine all the six unknown muscle force magnitudes $\{F\}$. To arrive at an unequivocal solution and to solve the indeterminacy of the system, additional information is therefore needed to constrain the possible solutions. The underlying strategy through which the muscles share to produce the required moments has been a source of debate in the literature [22, 23]. Two successive optimizations are utilized here. The first optimization is to specify $\{F^p\}$ such that the load evenly distributed over the muscles in order to minimize the sum of squared muscle stresses. This interpretation of load sharing requires contributions of all the involved muscles, which coincides with our EMG results [24]. Making use of Lagrange multipliers the analytical solution of the optimization is achieved

$$\{F^p\} = E^{-1}B^T(BE^{-1}B^T)^{-1}D \tag{7}$$

where $[E]_{6\times6}$ is a diagonal matrix with diagonal elements equal to $1/PCSA_j^2$. Physiological cross-sectional area ($PCSA_j$) is defined as the volume of the j^{th} muscle element divided by the corresponding optimal fiber length [25].

In order to achieve the complete solution to Eq. 5, the second optimization serves to define $\{F^s\}$ in the null space of $[B]$ such that the complete solution lies in the physiological operating domains of the muscles. Having defined $\{F^p\}$, the second optimization is outlined in Eq. 8, which can be solved with quadratic programing routines in Matlab®.

$$\begin{aligned} &\min(\boldsymbol{F}^p + N\boldsymbol{\mu})^T\ E\ (\boldsymbol{F}^p + N\boldsymbol{\mu}) \\ &\text{s.t.}\quad \mathbf{0} \le \boldsymbol{F}^p + N\boldsymbol{\mu} \le k\{PCSA\} \end{aligned} \tag{8}$$

where $\boldsymbol{\mu}$ is the decision variable and k is a scalar that linearly scales the maximum muscle force with $\{PCSA\}$ [25].

D. Model verification

CT scans of a non-pathological cadaver shoulder, performed in our laboratory [26], was utilized here as the set of anatomical data. In Fig. 3 the glenohumeral contact force (GHCF) obtained from the model was plotted along with the contact forces measured *in vivo* utilizing instrumented prosthesis, reported in [27]. The same slow abduction movement as what considered during the *in vivo* study was inputted to the model. Due to the individual differences amongst the six objects from whom the *in vivo* results were obtained, the *in vivo* contact forces vary subtly and were therefore represented as a gray shaded band. The GHCF predicted by the model agrees with the measured *in vivo* contact forces, which is partially ensured the validation of the model.

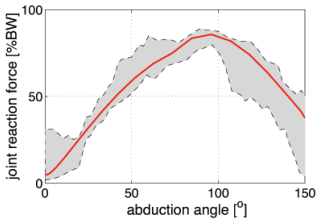

Fig. 3: GHCF predicted analytically (red line) along with *in vivo* results (gray band).

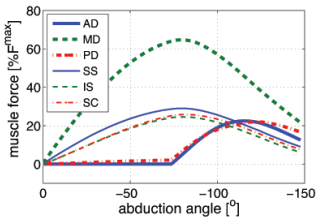

Fig. 4: contribution of muscles in slow abduction motion.

The contribution of different muscles surrounding the joint during the slow abduction motion is depicted in Fig. 4. These muscle forces are coherent with the results gained from EMG [24].

III. Stability Analysis and Results

A biomechanical interpretation to define the etiology behind the shoulder anterior instability is presented in this section. To this end, the role of joint active stabilizers is quantitatively assessed through vector analysis of the model results. A joint motion consists of 150° abduction along with 35° external rotation is utilized to expose the joint into the end-range where the anterior dislocation is more likely to occur.

The locus corresponding to the intersection of the muscles resultant force and the glenoid fossa are respectively depicted in Fig. 5 and Fig. 6 for the pure abduction and the combined abduction and external rotation motions.

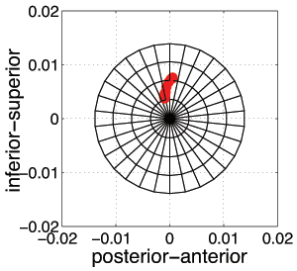

Fig. 5: locus during the pure abduction.

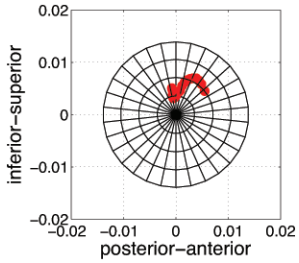

Fig. 6: locus during the combined abduction and external rotation.

According to Fig. 5 during the pure abduction the locus stay in central location and shifts subtly superiorly which is comparable to the previous clinical and cadaveric studies [28]. However, as illustrated in Fig. 6 the locus moves anteriorly by reaching the end-range postures, indicating gradual decline in the active stability, which can lead to anterior dislocation if the passive stabilizers are dysfunctional.

The contribution of different muscle groups toward the joint stability, during the combined abduction and rotation motion is assessed. To this end, the locus of the resultant forces produced by the rotator cuff muscles as well as the deltoid muscles are separately plotted in Fig. 7 and Fig. 8. The locus pertinent to the rotator cuff muscles moves anteriorly which expresses that their stabilizing function becomes less effective in the end-range. However, during the mid-range they are well aligned to not only compensate the destabilizing effects of deltoid muscles but also they act as the prime active stabilizers by compressing the humeral head into the glenoid fossa. Conversely, the locus corresponding to the deltoid muscles lie superoanteriorly even in the mid-range indicating their destabilizing effect as the main movers of the arm. The active anterior stability therefore diminishes in the end-range, which can lead to anterior dislocation if the passive structures are lax.

In Fig. 9 contributions of different muscles spanning the joint are highlighted making use of the concept of the balance stability angle introduced in [29]. The balance stability angle is defined by the angle between the center of the sphere approximates the glenoid and the end of the glenoid effective arc. The contributions of the muscles in anterior stability

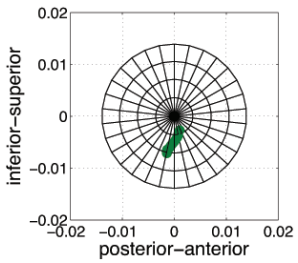

Fig. 7: locus corresponding to rotator cuff muscles.

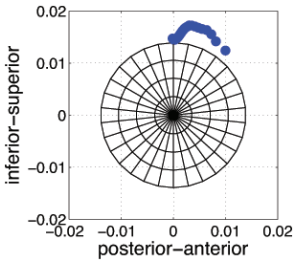

Fig. 8: locus corresponding to deltoid muscles.

were quantified here in terms of the angle that their lines of action make with the anterior-posterior direction.

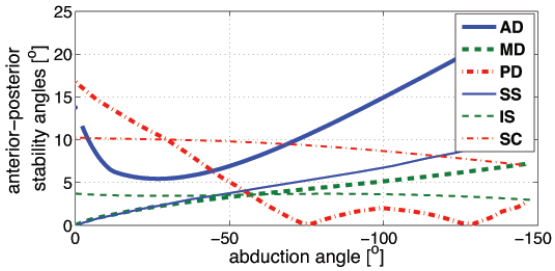

Fig. 9: variation of anterior-posterior balance angles.

The angles pertinent to the deltoid muscles are increased while the arm reaching the end-range postures, indicating that their lines of action point outward the fossa.

IV. Conclusion

The inherent instability of the glenohumeral joint was discussed and a rational biomechanical interpretation for the anterior instability, making use of vector analysis of the model results, was argued. It was illustrated that the active stability diminishes in the end-range postures which can lead to anterior dislocation if the passive stabilizers are dysfunctional. The anterior-posterior balance angles pertinent to the muscle forces were addressed to quantify the contribution of muscles toward stability and instability during the full range motion. The contributions of muscle groups were assessed through the locus of their line of action on the glenoid fossa. The active stabilizing role of the rotator cuff muscles become less effective during the end-range motions while the deltoid muscles act mainly as the movers during the full range.

The results of this study obtained through an inverse dynamic model along with assuming a constant dynamic for the muscle during the whole range. This can influence the accuracy of the results, as the muscles dynamic varies by the arm posture. A forward dynamic approach can therefore increase confidence of the results. Furthermore, considering dynamic interplay between the individual awareness of the joint position and the muscles line of action and magnitudes can influence the results. However existence of such feedback loop

is still a source of debate in the literature. The results can assist improving the treatment approaches developed for the anterior instability besides providing a deeper comprehension toward the contribution of different muscle groups during the task sharing.

ACKNOWLEDGMENT

This project was supported by the Swiss National Science Foundation [?-????-??????].

REFERENCES

1. Cutts Steven, Prempeh Mark, Drew Steven. Anterior shoulder dislocation. *Annals of the Royal College of Surgeons of England.* 2009;91:2–7.
2. Wilk, Kevin E., Christopher A. Arrigo James R. Andrews. Current concepts, the stabilizing structures of the glenohumeral joint.pdf 1997.
3. Veeger H E J, Helm F C T. Shoulder function: the perfect compromise between mobility and stability. *Journal of biomechanics.* 2007;40:2119–29.
4. Yanagawa Takashi, Goodwin Cheryl J, Shelburne Kevin B, Giphart J Erik, Torry Michael R, Pandy Marcus G. Contributions of the individual muscles of the shoulder to glenohumeral joint stability during abduction. *Journal of biomechanical engineering.* 2008;130:021024.
5. VandenBerghe Gregory, Hoenecke Heinz R., Fronek Jan. Glenohumeral Joint Instability: The Orthopedic Approach *Semin Musculoskelet Radiol.* 2005;09:34-43.
6. M.A. Zumstein MD, B. Jost MD C. Gerber MD. Instability of the Shoulder in Athletes in *Sportmedizin und Sporttraumatologie*:27–35 2005.
7. Hess S A. Functional stability of the glenohumeral joint *Manual therapy.* 2000;5:63–71.
8. Parsons I M, Apreleva Maria, Fu Freddie H, Woo Savio L. The effect of rotator cuff tears on reaction forces at the glenohumeral joint *Journal of Orthopaedic Research.* 2002;20.
9. Labriola Joanne E, Lee Thay Q, Debski Richard E, McMahon Patrick J. Stability and instability of the glenohumeral joint: the role of shoulder muscles. *Journal of shoulder and elbow surgery.* 2004;14:32S–38S.
10. Ackland David C, Pandy Marcus G. Lines of action and stabilizing potential of the shoulder musculature. *Journal of anatomy.* 2009;215:184–97.
11. Soslowsky, L. J., Flatow, E. L., Bigliani, L. U., Pawluk, R. J., Ateshian, G. A., & Mow V. C.. Quantitation of in situ contact areas at the glenohumeral joint: a biomechanical study *Journal of Orthopaedic Research.* 1992;10:524–534.
12. Strauss Eric J, Salata Michael J, Sershon Robert a, Garbis Nickolas. Role of the superior labrum after biceps tenodesis in glenohumeral stability. *Journal of shoulder and elbow surgery.* 2014;23:485–91.
13. Pagnani Michael J, Deng Xiang-hua, Warren Russell F, Torzilli Peter A, Brien Stephen J O. Role of the long head of the biceps brachii in glenohumeral stability : A biomechanical study in cadavera *Journal of shoulder and elbow surgery.* 1996:255–262.
14. Gohlke Frank, Essigkrug Bernhard, Schmitz Frank. The pattern of the collagen fiber bundles of the capsule of the glenohumeral joint *Journal of Shoulder and Elbow Surgery.* 1994;3:111–128.
15. Novotny John E, Beynnon Bruce D, Nichols Claude E. Modeling the stability of the human glenohumeral joint during external rotation *Journal of biomechanics.* 2000;33:345–354.
16. Alexander Susan, Southgate Dominic F L, Bull Anthony M J, Wallace Andrew L. The role of negative intraarticular pressure and the long head of biceps tendon on passive stability of the glenohumeral joint. *Journal of shoulder and elbow surgery.* 2013;22:94–101.
17. Braman Jonathan P, Engel Sean C, LaPrade Robert F, Ludewig Paula M. In vivo assessment of scapulohumeral rhythm during unconstrained overhead reaching in asymptomatic subjects *Journal of Shoulder and Elbow Surgery.* 2009;18:960–967.
18. Iannotti, J. P., & Williams G. R.. *Disorders of the shoulder: diagnosis & management (Vol. 1).* Lippincott Williams & Wilkins 2007.
19. Ingram David, Engelhardt Christoph, Farron Alain, Terrier Alexandre, Müllhaupt Philippe. Muscle moment-arms: a key element in muscle-force estimation *Computer methods in biomechanics and biomedical engineering.* 2013:37–41.
20. Marsden S P, Swailes D C, Johnson G R. Algorithms for exact multi-object muscle wrapping and application to the deltoid muscle wrapping around the humerus *Proceedings of the Institution of Mechanical Engineers, Part H: Journal of Engineering in Medicine.* 2008;222:1081–1095.
21. Baruh H.. *Analytical dynamics*. Boston: WCB/McGraw-Hill 1999.
22. Brinckmann, P., Frobin W.. *Musculoskeletal biomechanics*. Thieme 2002.
23. Praagman M, Chadwick E K J, Helm F C T, Veeger H E J. The relationship between two different mechanical cost functions and muscle oxygen consumption. *Journal of biomechanics.* 2006;39:758–65.
24. Engelhardt Christoph, Malfroy Camine Valérie, Ingram David, et al. Comparison of an EMG-based and a stress-based method to predict shoulder muscle forces *Computer methods in biomechanics and biomedical engineering.* 2014;(ahead-of-:1–8.
25. Bamman, M. M., Newcomer, B. R., Larson-Meyer, D. E., Weinsier, R. L., & Hunter G. R.. Evaluation of the strength-size relationship in vivo using various muscle size indices *Medicine and science in sports and exercise.* 2000;32:1307–1313.
26. Terrier Alexandre, Reist Adrian, Vogel Arne, Farron Alain. Effect of supraspinatus deficiency on humerus translation and glenohumeral contact force during abduction. *Clinical biomechanics (Bristol, Avon).* 2007;22:645–51.
27. Bergmann G, Graichen F, Bender a, et al. In vivo gleno-humeral joint loads during forward flexion and abduction. *Journal of biomechanics.* 2011;44:1543–52.
28. Bey Michael J, Kline Stephanie K, Zauel Roger, Kolowich Patricia a, Lock Terrence R. In Vivo Measurement of Glenohumeral Joint Contact Patterns *EURASIP journal on advances in signal processing.* 2010;2010:2–7.
29. Rockwood Jr, C. A., Matsen , F. A., Wirth, M. A., Lippitt S. B.. *The shoulder*. Elsevier Health Sciences 2009.